

Hydrological Behaviour of Microbiotic Crusts on Sand Dunes of NW China: Experimental Evidences and Numerical Simulations

Antonio Coppola¹, Anna Tedeschi, Angelo Basile and Massimo Menenti

CNR-ISAFOM. Institute for Mediterranean Agro Forestry Systems
Via Patacca 85, 80056 Ercolano Naples, ITALY
E-mail: ¹antonio.coppola@unibas.it

Xinping Wang

Cold & Arid Regions Environmental & Engineering Research Institute
Chinese Academy of Sciences, 260 West Donggang Road, Lanzhou 730000, CHINA

Vincenzo Comegna and Antonio Coppola

University of Basilicata, Dept. for Agro-Forestry Systems Management (DITEC)
viale dell'Ateneo Lucano, 85100 Potenza, ITALY

ABSTRACT: Large ecological engineering projects were established to reduce and combat the hazards of sandstorms and desertification in northern China. An experiment to evaluate the effects of dunes stabilization by vegetation was carried out at Shapotou in Ningxia Hui Autonomous Region at the southeast edge of the Tengger Desert using xerophyte shrubs (*Caragana korshinskii*, *Hedysarum scoparium* and *Artemisia ordosica*) planted in straw checkerboard plots in 1956, 1964, 1981, 1987, 1998 and 2002. The fixed sand surface led to the formation of biotic soil crusts. Biotic crusts formed at the soil surface in the interspaces between shrubs and contribute to stabilization of soil surfaces. Previous results on the area have showed that: i) straw checkerboards enhance the capacity of the dune system to trap dust, leading to the accumulation of soil organic matter and nutrients; ii) the longer the period of dune stabilization, the greater the soil clay content in the shallow soil profile (0-5 cm), and greater the fractal dimension of soil particle size distribution. Benefit apart, one should be aware that the formation of a crusted layer at the soil surface is generally characterized by an altered pore-size distribution, with a frequent decrease of hydraulic conductivity which can induce changes of the water regime of the whole soil profile. Accordingly, the main objective of the paper is to evaluate the equivalent (from a hydraulic point of view) geometry of the crusted layer and to verify if the specific characteristics of the crusted soil layer, although local by nature, affect the hydrological behaviour of the whole soil profile. In fact, it is expected that, due to the formation of an upper, impeding soil layer, the lower soil layers do not reach saturation. Such behaviour has important consequences on both water flow and storages in soils. The final aim will be to understand how the crust at the surface of the artificially stabilized sand dune affects the infiltration capacity at the soil surface and how, in turn, this affects the soil water content profiles.

INTRODUCTION

Crusting of the soil surface has been observed in many parts of the world in soils with different textures. Generally, crust formation occurs under the influence of rain storm and drying weather. In this type of crust a disturbed level of variable thickness, illuviated by the material in suspension, follows a very superficial real crust. The disturbed layer can be characterized by vertical dishomogeneity in porosity, with a progressive transition towards the properties of the lower undisturbed layer.

Less understood and discussed is how the presence of biological soil crusts (consisting of soil surface cyanobacteria, green algae, microfungi, lichens and

bryophytes) (Belnap, 2006) influence local hydrological behavior. Biotic crusts form at the soil surface of arid and semiarid land in the interspaces between shrubs and contribute to stabilization of soil surfaces. To the contrary, the effect of biotic crusts on soil hydrology is often contradictory.

Biotic crusts are often associated to rain-induced crusts, which are known to restrict soil water infiltration. Nevertheless, the biotic-physical interaction produces crusts with atypical characteristics, compared to the classical rain-induced crusts, as they can imbibe water and swell, thus potentially restricting water flow along the soil profile. On the other side, as pointed out by Belnap and Gardner (1993), the additional structure provided by the microbiotic activity via soil carbon

addition would enhance the hydraulic conductivity rather than reduce it through new micropore channels (Eldridge *et al.*, 2001).

In arid north-west China, changes in landscape from desert dunes to artificially stabilized shrub-covered dunes strongly enhanced the formation of biotic crusts.

Studies by Wang *et al.* (2006) showed that this could result in a reduction of soil water replenishment, especially important where groundwater does not support the natural vegetation cover. In these conditions, the local hydrological regime might change significantly.

Until recently, limited and contradictory research has been conducted to determine the influence of biotic crusts on soil hydrological processes. To partially fill the gap, this study aims (i) to measure on different sites the soil physical and hydraulic properties of biotic crusts commonly found in an arid area of the north-west China and (ii) to evaluate the effects of these measured properties on the hydrological behavior of these soils by numerically simulating water flow processes naturally occurring in the area. The final aim will be (iii) to establish if and how the biotic crust affects the soil water storages and deep water fluxes in these crusted soil profiles.

MATERIALS AND METHODS

Study Site

This study was conducted in the Shapotou region, which is located in Zhongwei County in the Ningxia Hui Autonomous Region at the southeastern edge of the Tengger Desert (37° 32' N, 105° 02' E). It is an ecotone between steppified desert and desertified steppe and also a transitional zone between sandy desert and oasis (Li *et al.*, 2002, Shapotou Desert Research and Experiment Station, CAS, 1991). Natural vegetation in the sandy desert region is dominated by the psammophytes, such as *Hedysarum scoparium* Fisch., *Agriophyllum squarrosum* Moq., *Stilpnolepis centiflora* Krasch and *Pugionium calcaratum* Kom., etc, with coverage of about 1% (Li *et al.*, 2003). Based on long-term measurements from 1955 to 2001, the mean temperature in January is -6.1°C and in July 24.7°C. Mean relative humidity varies from 31% (April) to 54% (August). The first frost occurs in late September and the last frost ends in mid April. The annual mean precipitation is 191 mm and about 80% of this falls between June and September. The annual class A pan evaporation is about 2400 mm. The area has large and dense reticulate dune chains. The main

dune crest migrates southeastward at a velocity of 0.3–0.6 m year⁻¹. The soil is loose and impoverished mobile sand classified as Typic Psammaquents (Berndtsson *et al.*, 1996). The groundwater is between 50 and 80 m and, therefore, is unable to support the natural vegetation. Rainfall is the only source of fresh water. The natural predominant plants are *Hedysarum scoparium* and *Agriophyllum squarrosum* with a cover of approximately 1–2% (Shapotou Desert Experimental Research Station, Chinese Academy of Sciences, 1991). A 16 km long vegetated protection system was established in the 1950's. Initially, a sand barrier was established with woven willow branches or bamboos to reduce wind erosion. Behind the sand barrier, straw chequerboards (wheat or rice straw) were installed, usually with sections of 1 m² area. The straw structures remain intact for 4–5 years, facilitating the establishment of planted xerophytic shrubs typical in this highly eroded environment (Wang *et al.*, 2006). The fixed sand surface has led to the formation of microbiotic soil crusts. Details on the soil composition analysis of the stabilized dune sand with and without microbiotic soil crust can be found in Wang *et al.* (2006).

Measurements

Infiltration measurements were performed by a tension disc infiltrometer (Ankeny *et al.*, 1991) with a 20 cm-diameter disc, covered with a highly permeable nylon membrane. Infiltration measurements were performed at laboratory-calibrated supply potential of -1, -4, -7, -10, -18 cm. Each sequence of infiltration runs at a given location started with the smallest supply potential, increasing stepwise to the largest potential. The transient infiltration was monitored until steady state conditions were reached. For each site, infiltration tests were carried out on crusted surface as well as on underlying sandy soil (by removing the surface crust) in order to estimate the contrast of infiltration behavior between crust and subsoil.

For each replicate site soil crust samples were collected for subsequent micro-morphological and stability of soil structure analyses to be carried out at the ISAFoM laboratories. The final aim was to completely characterize soil crusts in terms of pore geometry, structure and related hydrological properties.

Six sites were selected for carrying out the infiltration measurements. Information on sites and infiltration measurements for the six selected soils are given in Table 1.

Table 1: Number of Infiltration Tests for the Different Sites Investigated

Site	N. of Hor. (a)	Altitude (m)	Replicate Inf. Sequences (b)	Tension Step Sequence (c)	Total Data Points (a * b * c)
Hongwei	2	1583.62	2	4	16
Water Balance	2	1211.83	2	4	16
Yi Wan Quan	2	1671.33	2	3-4	15
Railway 1956	2	N.A.	2	3-4	15
Railway 1964	2	N.A.	2	4	16

At the beginning and at the end of each infiltration measurements sequence soil samples were collected in order to determine the initial and final water contents.

Data Handling

Hydraulic conductivity was estimated from Wooding’s solution (1968) for steady-state flow from a shallow circular pond. It assumes that flow is described by Darcy’s equation and that soil is uniform with initial water potential, h_n , and volumetric water content θ_n . The soil is dry initially with h_n tending to $-\infty$ and hydraulic conductivity $K(h_0)$ is given by the quasi-linear Gardner model (Gardner, 1958),

$$K(h_0) = K_{fs} \exp(\alpha_{GRD} h_0) \quad \dots (1)$$

where $K(h_0)$ is the unsaturated conductivity at a given pressure head h_0 , K_{fs} the field-saturated hydraulic conductivity and α_{GRD} is the exponential slope.

Herein, with the term saturation we mean the maximum water content we were able to obtain according to the experimental saturation procedures we used.

Wooding’s solution for infiltration from a circular source with a constant pressure head at the soil surface and with the unsaturated hydraulic conductivity described by Eqn. (1) is given by,

$$Q(h_0) = \left(\pi r_0^2 + \frac{4r_0}{\alpha_{GRD}} \right) K(h_0) \quad \dots (2)$$

where $Q(h_0)$ is the steady-state infiltration rate at the supply pressure head h_0 imposed, r_0 is the radius of the disc, $K(h_0)$ and α_{GRD} are the same as in Eqn. (1). The first term on the right-hand side represents the effect of gravitational forces and the second term the effect of capillary forces. Analysis of tension disc infiltrometer data was made following the multiple head approach that requires two or more steady-state flow values for a single disc radius at different pressure heads to obtain a piecewise relationship $K(h_0)$ (Ankeny *et al.*, 1991; Jarvis and Messing, 1995).

The approach assumes that parameter α_{GRD} in Eqn. (1) is constant over the interval between two adjacent supply pressure heads such that,

$$\alpha_{GRDi+1/2} = \frac{\ln \frac{Q_i}{Q_{i+1}}}{h_i - h_{i+1}} \quad i = 1, \dots, n-1 \quad \dots (3)$$

where n is the number of supply pressure heads used. The notation $\frac{1}{2}$ denotes the estimated value of α_{GRD} at the midpoint between successive supply pressure heads. The infiltration rate $Q_{i+1/2}$ at the half-way point between two adjacent supply pressure heads $h_{i+1/2} = (h_i + h_{i+1})/2$ is calculated as a geometric mean of the actual infiltration rates Q_i and Q_{i+1} . Therefore, the unsaturated hydraulic conductivity at $h_{i+1/2}$ can be calculated as,

$$K_{i+1/2} = \frac{Q_{i+1/2}}{\pi r^2 + \frac{4r}{\alpha_{GRDi+1/2}}} \quad i=1, \dots, n-1 \quad \dots (4)$$

Another two values of $K(h_0)$ can be obtained if we assume that the values of α_{GRD} at the largest and smallest pressure heads are equal, respectively, to $\alpha_{GRD3/2}$ and $\alpha_{GRDn-1/2}$.

Finally, assuming the slope of the curve to be constant from the last measured value and the saturated hydraulic conductivity, K_s is calculated from Eqn. (1) using known values of $h_{i+1/2}$, $K_{i+1/2}$, and $\alpha_{GRDi+1/2}$ as follows,

$$K_s = \frac{K_{i+1/2}}{\exp(\alpha_{GRDi+1/2} h_{i+1/2})} \quad i=1, \dots, n-1 \quad \dots (5)$$

In order to deduce simultaneously the water retention and hydraulic conductivity curves from the same infiltration experiment, in this study, the results from the Wooding’s analysis were coupled to a parameter estimation method based on a numerical solution of the Richard’s equation (Lazarowitch *et al.*, 2007).

The governing equation for radial symmetric isothermal water flow in an unsaturated rigid soil is given by the following modified form of the Richards equation (Warrick, 1992),

$$\frac{\partial \theta}{\partial t} = \frac{1}{r} \frac{\partial}{\partial r} \left(rK \frac{\partial h}{\partial r} \right) + \frac{\partial}{\partial z} \left(K \frac{\partial h}{\partial z} - 1 \right) \quad \dots (6)$$

where t is time, z is the vertical coordinate taken positive downwards, K is hydraulic conductivity, h is pressure head, and r is the radial coordinate.

Equation (6) can be solved numerically when the initial and boundary conditions are prescribed and the soil water retention, $\theta(h)$, and hydraulic conductivity, $k(\theta)$, functions are specified. We used the van Genuchten (1980) analytical expression to describe the soil water retention,

$$S_e = \frac{\theta - \theta_r}{\theta_s - \theta_r} = \left[1 + |\alpha_{VG} h|^n \right]^m \quad h < 0 \quad \dots (7)$$

$$\theta = \theta_s \quad h \geq 0$$

where S_e is effective saturation, α_{VG} (cm^{-1}), n and m are shape parameters, θ_s and θ_r are the saturated and residual water content, respectively. Combined with the statistical pore-size distribution model for the unsaturated hydraulic conductivity of Mualem (1986), with the restriction $m = 1 - 1/n$, an analytical expression for the $k(\theta)$ curve becomes,

$$k_r(S_e) = \frac{k(S_e)}{k_s} = S_e^\tau \left[1 - \left(1 - S_e^{1/m} \right)^m \right]^2 \quad \dots (8)$$

in which k_r is the relative hydraulic conductivity, and τ is a parameter which accounts for the dependence of the tortuosity and the correlation factors on the water content.

The transient experimental infiltration data, along with initial and final water content, were used for the numerical inverse approach, by fixing saturated hydraulic conductivity to the value obtained from the Wooding's analysis. The unsaturated hydraulic conductivity experimental points calculated by the Wooding's analysis were used to validate the inversion results.

Hydrological Simulations

The influence of the biological crust on water flow processes in the soil profiles was investigated using a numerical code written in MATLAB. A full description is given by Coppola and Randazzo (2006). One-dimensional vertical transient water flow in this

model is simulated by numerically solving the 1D form of the Richards equation (Eqn. 9) using an implicit, backward, finite differences scheme with explicit linearization similar to that adopted in the SWAP model (van Dam *et al.*, 1997),

$$C(h) \frac{\partial h}{\partial t} = \frac{\partial}{\partial z} \left(k(h) \frac{\partial h}{\partial z} - k(h) \right) - S(h) \quad \dots (9)$$

where $C(h) d\theta/dh$ is the soil water capacity, h is the soil water pressure head, t is time, z is the vertical coordinate being positive upward, $k(h)$ the hydraulic conductivity and $S(h)$ is a sink term describing water uptake by plant roots. Several water retention and hydraulic conductivity models can be selected. In this study we assumed that the soil hydraulic properties can be described by the unimodal van Genuchten-Mualem model as described above. Flow rates and pressure heads, whether constant or variable over time, can be assumed as the upper boundary condition. Gradients of different value, pressure heads or flow rates, again whether constant or variable, can be assumed at the bottom of the soil profile.

Biological soil crust organisms grow to unknown depths in the soil profile. However, the highest concentration of microbiotic activity and associated concentration of silt and clay is within the first 5 cm of the soil surface (Williams *et al.*, 1999). Previous analyses of particle size distribution of the examined soils (Wang *et al.*, 2006) showed that at a soil depth of 0–5 cm, the stabilized dune sand with microbiotic soil crust contained the largest amount of fine soil particles in the range of 0.002–0.25 mm, the largest organic matter content, compared to the uncrusted soil. The organic matter content and bulk density displayed significant differences between the different surface. At the soil depth of 10–20 cm no differences were found. Thus, in this study, two main layers (0–5 cm (crust) and 5–100 cm (sand)) were considered. The hydrological behavior of the soil profile with and without crust was compared. Meteorological data were obtained from a remotely controlled micrometeorological station located close to the experimental sites. Simulations conducted in this paper refer to a time interval of about 100 days characterized by the occurrence of a sparse series of rainfall events.

RESULTS AND DISCUSSION

Measurement Results

In Figures 1(a), (b) water retention and hydraulic conductivity curves are shown. Simple solid lines are

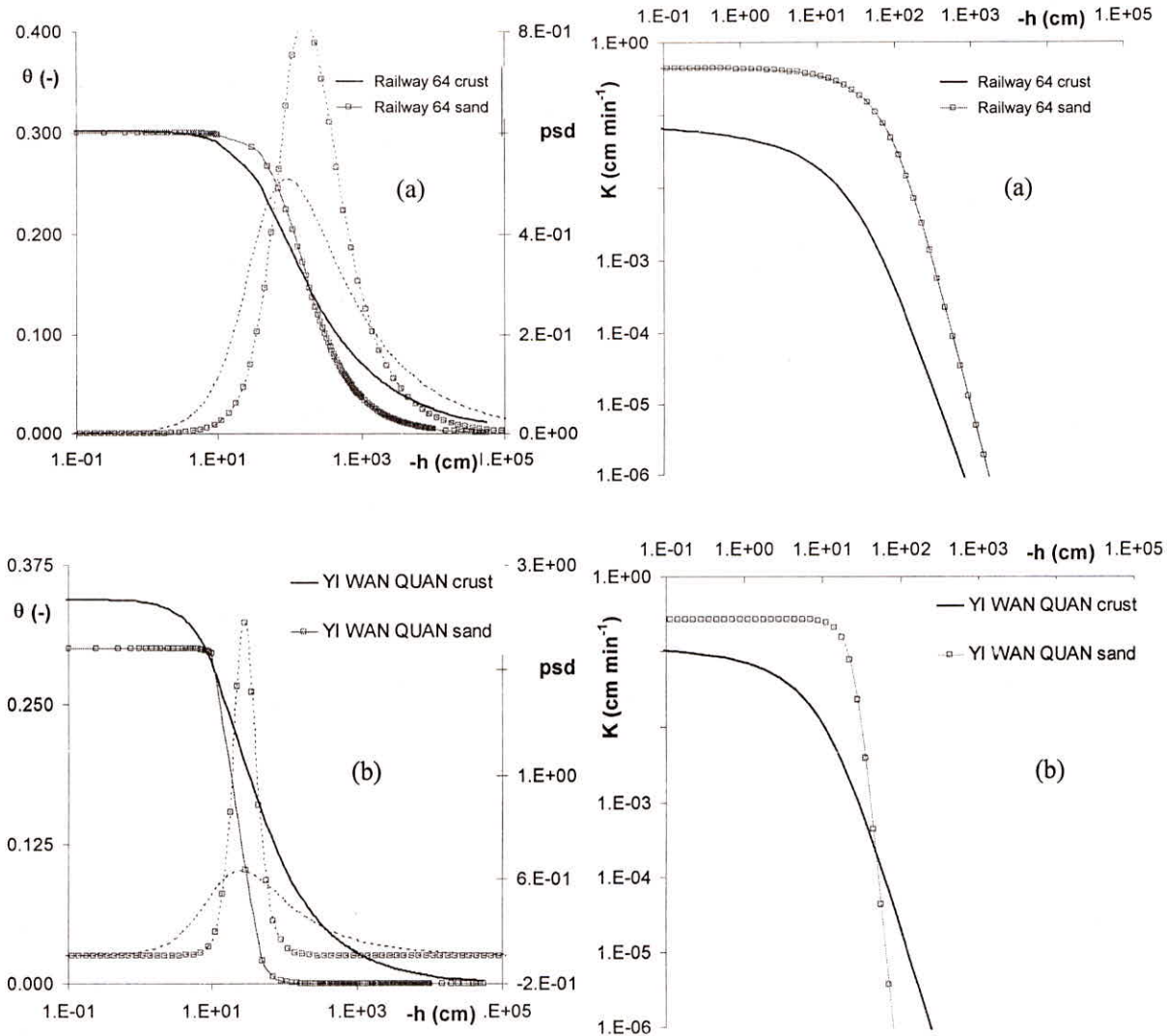


Fig. 1(a), (b): Water retention, hydraulic conductivity and pore-size distributions for the two soil sites examined

for the crust layer while solid lines and symbols are for the sand layer. Dashed lines represent the corresponding equivalent pore size distribution (pdf). Again, lines plus symbols indicate the sandy subsoil.

Two different sites were compared (*Railway 64* and *Yi Wan Quan*), in order to show the impact of different time of crusting (1964 for *Railway 64* site and a few years for *Yi Wan Quan* site).

The pdf were estimated from the retention curves as follows,

$$f(h) = \frac{d\theta(h)}{d \log_{10} h} = \frac{[\log_e 10] h d\theta(h)}{dh} \quad \dots (10)$$

Comparison of curves shows higher water retention for lower values of the pressure head. For the higher values of the pressure head water retention remains unaltered (*Railway 64*) or even improved (*Yi Wan*

Quan) while the hydraulic conductivity decreases, both in the saturated and unsaturated medium for the *Railway 64* site, for the crust layer in response to a change in pore distribution; as expected, the latter widens and shows a reduced peak. Increasing of water retention and decreasing of the hydraulic conductivity can be explained by considering the peculiarity of biological crusts, compared to the rain-induced crusts. As pointed out by Belnap (2006), dry crust microphytes swell upon wetting as they imbibe water, so that water retention increases but soil hydraulic conductivity can be restricted.

HYDROLOGICAL SIMULATION RESULTS

The graph in Figures 2(a), (b) represent the evolution of simulated water contents at two different depths (2.5 cm and 40 cm), for the two sites examined (*Railway 64* – Figure 2(a) and *Yi Wan Quan* – Figure 2(b)).

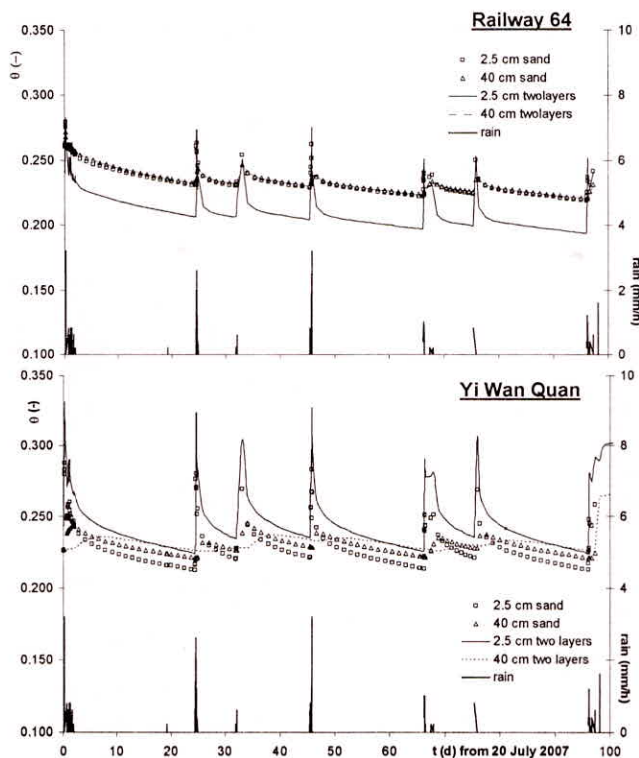


Fig. 2(a), (b): Water contents simulated at 2.5 cm and 40 cm for Railway (a) and Yi Wan Quan (b) sites

Open symbols and lines in Figure 2 represent simulated water contents for the case of a one-layer profile (sand without crust), and a two-layers soil profile (crust above sand), respectively.

Both the graphs show in detail the fast response of the water content to rainfall and evaporating demand.

Concerning the 2.5 cm depth, the evolution of water content for the crust and for the subsoil follows a very similar shape. For the Railway 64 site the crust water content values are shifted downward for the lower pressure head values while they are of the same magnitude during rainfall events. This response is only obvious due to the specific behavior of the pertaining retention curve (see Figure 1(a)). By arguing for analogy, for the Yi Wan Quan site the water content of the crusted soil is always higher than that of the uncrusted soil at 2.5 cm due again to the water retention curve shapes for that site (see Figure 1(b)).

The 40 cm water content curves obtained on the two sites are, with due proportions, almost equivalent, thus confirming the goodness of the hydraulic characterizations on which the simulations are based. Interestingly, the water content at 40 cm remains unaffected by the presence of the crust, for both sites. Similar results can be observed looking at the Figures 3(a), (b) showing the storages calculated at 40 cm and 100 cm depth and

the Figures 4(a), (b) showing fluxes calculated at 100 cm depth. Once again, open symbols and lines represent simulations for the case of a one-layer profile (sand without crust), and a two-layers soil profile (crust above sand), respectively.

Note the quasi-equivalent storages obtained for both the sites though with a different trend in the 100 cm water fluxes.

Although this behavior may appear unexpected due to the different hydraulic conductivities for the crust and the sand, it can be easily explained if one consider that the lower hydraulic conductivities in the crust are counteracted by increasing hydraulic gradients at the crust-sand interface. This, in turn, results in equivalent fluxes from the interface downward for both the crusted and uncrusted profiles, so that roughly equal storages are also obtained, with the exception of the first (irrelevant) 5 cm. This results has practical direct implications as the microbiotic crust stabilizes soil surface without interfering with the soil water balance. This contradicts the general thought that any crust should be seen as an impeding thin layer affecting the hydrological behavior of the whole soil profile. Of course, this behavior can only be ascribed to the specific rainfall regime of the area, with infrequent rainfalls which only rarely saturate the soil surface.

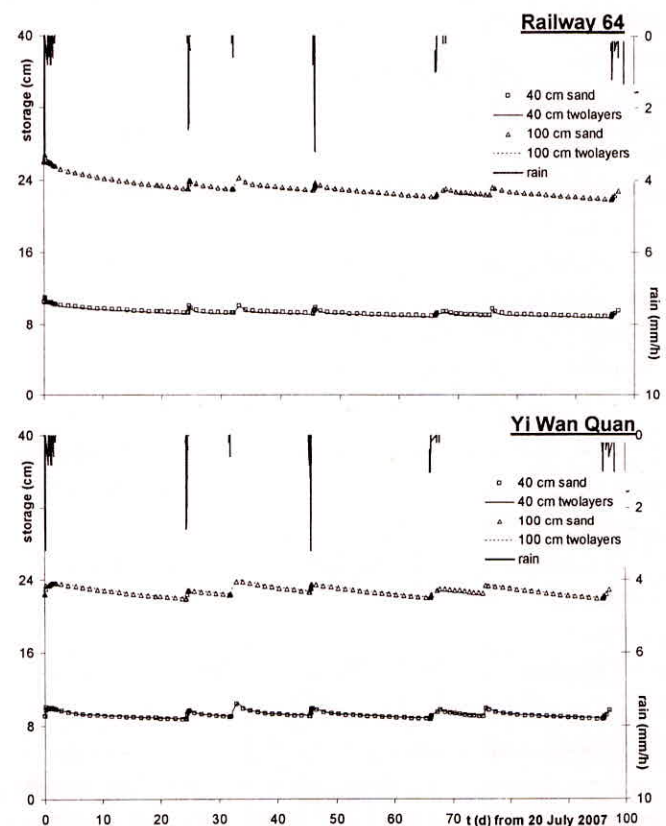


Fig. 3(a), (b): Storages simulated at 100 cm depth

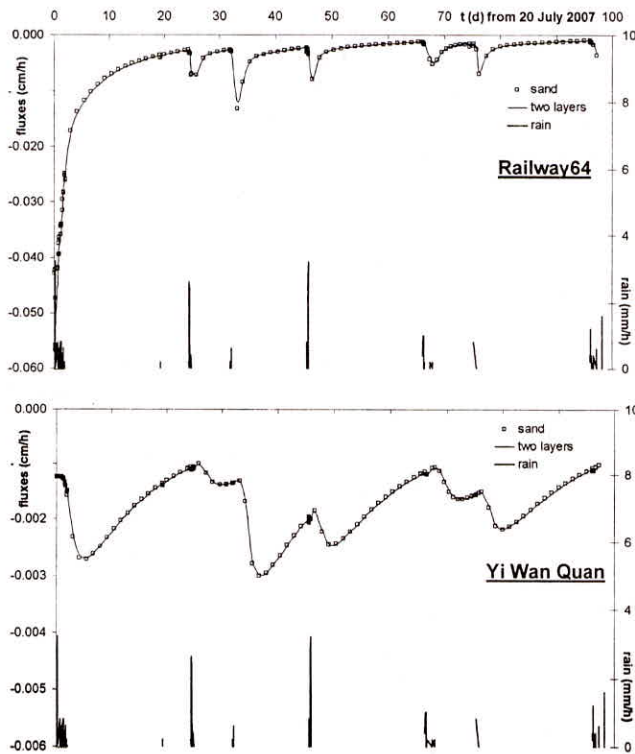


Fig. 4(a), (b): Water fluxes simulated at 100 cm depth

This can be easily observed in Figure 5(a), (b), which report, for the Railway 64 site, the comparison between the spatial-temporal distributions of the pressure heads pertaining to the crusted (a) and uncrusted (b) 100 soil profiles simulated by imposing a pressure head at the surface $h = -3$ cm and a unit hydraulic gradient as bottom boundary condition. While the wetting front propagates unchanged up to 100 cm in the homogeneous sand medium (Figure 5(b)), saturating the whole soil profile, the changed conditions of the medium on the surface after crusting (decrease in hydraulic conductivity, change in retention parameters) are matched by pressure head values in the layer immediately below the disturbed surface which are far from zero, indicating that only partial saturation of the porous medium has been reached (Figure 5(a)). Of course, the corresponding water contents are always lower than the maximum reached in the uncrusted profile, so that deep fluxes and storages are also expected to change significantly. Formation of a disturbed level at the profile surface, of a relatively modest thickness, thus ends up conditioning the whole soil water regime.

CONCLUSIONS

The effect of microbiotic crusts on local hydrologic regime of the investigated soils was evaluated. The biotic-physical interaction at soil surface is unlike the

transient seal formed by raindrop splash has the former may well upon wetting thus inducing contradictory water retention and hydraulic conductivity changes. As for the rain-induced crusts, for persistent high pressure head values at the soil surface, the changes occurring in the biotic crusted soil layer, although local by nature, were shown to affect the hydrological behavior of the whole soil profile. Specifically, we provided evidences that the main physical and hydrological consequences occurring locally (namely: decrease in both saturated and unsaturated hydraulic conductivity) always cause unsaturated fluxes in the soil beneath the disturbed layer and, consequently, also lower water storages are expected. Under these conditions, the biotic crust has to be considered an impeding layer. Nevertheless, for the actual rainfall water regimes, it has insignificant effects on the local soil water regime, with unchanged storages and deep fluxes.

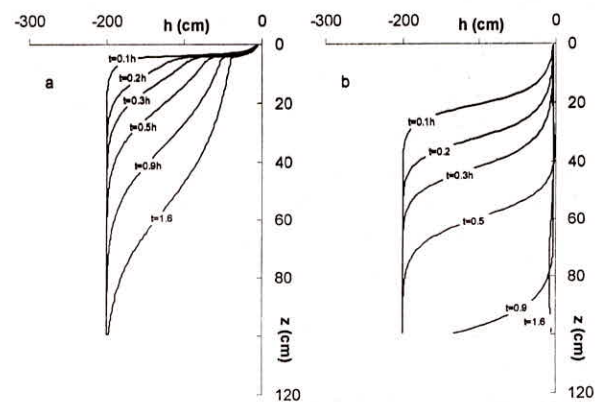


Fig. 5: Comparison between simulated pressure head distributions pertaining to the crusted (a) and uncrusted (b) hydraulic characterizations for the Railway 64 site

ACKNOWLEDGEMENTS

This research was supported by the scientific bilateral cooperation 2004–2007 between CNR/Chinese Academy of Science and by the Short Term Mobility program funded by CNR, 2007. Moreover the National Natural Science Foundation of China, supported the research project “The heterogeneity hydraulic characteristics of biological soil crusts and its influence on infiltration and evaporation processes”.

REFERENCES

Ankeny, M.D., Ahmed, M., Kaspar, T.C. and Horton, R. (1991). “Simple field method for determining unsaturated hydraulic conductivity.” *Soil Sci. Soc. Am. J.* 55:467–470.
 Belnap, J, Gardner, J.S. (1993). “Soil microstructure in soils of the Colorado Plateau: the role of the cyanobacterium *Microcoleus vaginatus*.” *Great Basin Naturalist* 53: 40–47.

- Belnap, J. (2006). "The potential roles of biological soil crusts in dryland hydrologic cycles." *Hydrol. Process.* 20, 3159–3178, DOI: 10.1002/hyp.6325.
- Berndtsson, R., Nodomi, K., Yasuda, H., Persson, T., Chen, H. and Jinno, K. (1996). "Soil water and temperature patterns in an arid desert dune sand." *Journal of Hydrology* 185: 221–240.
- Coppola, A. and Randazzo, L. (2006). "A MathLab code for the transport of water and solutes in unsaturated soils with vegetation." *Tech. Rep. Soil and Contaminant Hydrology Laboratory*, Dept. DITEC University of Basilicata.
- Eldridge, D.J., Lepage, M., Bryannah, M.A. and Ouedraogo, P. (2001). "Soil biota in banded landscapes." In *Banded Vegetation Patterning in Arid and Semiarid Environments: Ecological Processes and Consequences for Management*, Tongway, D.J., Valentin, C., Seghieri, J. (eds). Springer-Verlag: New York; 105–131.
- Jarvis, N.J. and Messing, I. (1995). "Near-saturated hydraulic conductivity in soils of contrasting texture measured by tension infiltrometers." *Soil Sci. Soc. Am. J.* 59:27–34.
- Lazarowitch, N., Ben-Gal, A., Simunek, J. and Shani, U. (2007). "Uniqueness of soil hydraulic parameters determined by a combined Wooding inverse approach." *Soil Sci. Soc. Am. J.*, 71:860–865.
- Li, X.R., Wang, X.P., Li, T. and Zhang, J.G. (2002). "Microbiotic soil crust and its effect on vegetation and habitat on artificially stabilized desert dunes in Tengger Desert, north China." *Biology and Fertility of Soils* 35: 147–154.
- Li, X.R., Zhou, H.Y., Wang, X.P., Zhu, Y.G. and O'Conner, P.J. (2003). "The effects of sand stabilization and revegetation on cryptogam species diversity and soil fertility in the Tengger Desert, northern China." *Plant and Soil* 251: 237–245.
- Mualem, Y. (1986). "Hydraulic conductivity of unsaturated soils: Prediction and formulas." In *Methods of soil analysis, Part 1, Physical and mineralogical methods*. Klute, A. (ed.), 2nd ed. Agronomy 9(2). American Society of Agronomy. Madison, Wisconsin, pp. 799–823.
- Shapotou Desert Experimental Research Station, Chinese Academy of Sciences (1991). "Study on Shifting Sand Control in Shapotou Region of the Tengger Desert" (2). Ningxia People's Publishing House: Yingchuan; 101–119 (in Chinese with English abstract).
- Van Dam, J.C., Huygen, J., Wesseling, J.G., Feddes, R.A., Kabat, P., van Walsum, P.E.V., Groenendijk, P. and van Diepen, C.A. (1997). SWAP version 2.0, Theory. "Simulation of water flow, solute transport and plant growth in the Soil-Water-Atmosphere-Plant environment." *Technical Document* 45, DLO Winand Staring Centre, Report 71, Department Water Resources, Agricultural University, Wageningen.
- Van Genuchten MTh. (1980). "A closed-form equation for predicting the hydraulic conductivity of unsaturated soils." *Soil Sci. Soc. Am. J.* 44: 892–898.
- Wang, X.P., Li, X.R., Xiao, H.L., Berndtsson, R. and Pan, Y.X. (2006). "Effects of surface characteristics on infiltration patterns in an arid shrub desert." *Hydrol. Process.* DOI: 10.1002/hyp.6185.
- Warrick, A.W. (1992). "Models for disc infiltrometer." *Water Resour. Res.*, 28: 1319–1327.
- Williams, J.D., Dobrowolski, J.P., West, N.E. (1999). "Microbiotic crust influence on unsaturated hydraulic conductivity." *Arid Soil Research and Rehabilitation*, 13: 145–154.
- Wooding, R.A. (1968). "Steady infiltration from a shallow circular pond." *Water Resour. Res.* 4: 1259–1273.